

# The Effects of Proline Isomerization on the Solvation Behavior of Elastin-Like Polypeptides in Water–Ethanol Mixtures

Yani Zhao and Kurt Kremer\*

Elastin-like polypeptides (ELPs) are well-known proline-rich stimulus-responsive polymers. They have broad applications ranging from drug delivery to green chemistry. Recently, the authors have shown that the *cis/trans* proline isomerization can be used to regulate their conformational behavior while keeping the lower critical solution temperature (LCST) unchanged in pure water. In aqueous ethanol mixtures, ELPs typically exhibit an expanded–collapsed–expanded transition known as the co-non-solvency phenomenon. Since it is unclear how proline isomerization affects the solvation behavior of ELPs in aqueous ethanol mixtures, an all-atom insight on single ELPs has been provided to address this question. It is found that if all proline residues are in the *cis* state, the peptides only experience a collapsed–expanded transition as ethanol concentration increases, i.e., the initial collapse vanishes because *cis* isomers prefer the compact structures in pure water. The data from the authors also suggest that proline isomerization does not change the shift in solvation free energy of an ELP with given sequence, but it varies the affinity of the peptide to both the solvent and cosolvent molecules.

with a rather high energy barrier of about  $30\text{--}32 k_B T$ ,<sup>[6,7]</sup> though the Gibbs free energy difference between the two proline isomers is only  $\approx 2 k_B T$ .<sup>[6,8]</sup> Moreover, one has to note that there are a number of ways to catalyze the *cis/trans* isomerization or to enhance the *cis* content.<sup>[6,8–11]</sup>

For proline-rich stimulus-responsive peptides such as the Elastin-like polypeptides (ELPs) (a known class of stimulus-responsive peptide-like polymers with sequence Val-Pro-Gly-Xaa-Gly (VPGXG) in which Xaa can be any non-proline amino acid<sup>[12–14]</sup>), our previous work<sup>[15]</sup> has shown that proline isomerization can be applied to regulate their conformational behavior (the schematic representation of the *cis/trans* isomers is shown in Figure S1 in the Supporting Information and the corresponding  $\omega$  dihedral angle of the Val-Pro bonds can be found in our previous work<sup>[15]</sup>). In that paper, we have studied an ELP sequence of (VPGVG)<sub>30</sub> in pure water, and found that it

exhibited a first-order-like lower critical solution temperature (LCST) transition. This expanded–collapsed conformational transition as temperature  $T$  increases occurs if all of its prolines are in the *trans* state, while it remained rather collapsed at all considered temperatures if all prolines are in the *cis* state. In summary, our data have suggested that proline isomerization plays an important role in tuning the conformational behavior of ELPs in pure water while keeping their transition temperature  $T_i$  unchanged.

As many other stimulus-responsive polymers (also known as smart polymers<sup>[16–18]</sup>), ELPs exhibit rich and tunable phase diagrams also in aqueous binary mixtures. For example, in water–alcohol solutions, a co-non-solvency phenomenon of ELPs has been observed both experimentally<sup>[19]</sup> and computationally.<sup>[20]</sup> This phenomenon is associated with the collapse of the polymer in two miscible good solvents, i.e., the polymer experiences the expanded–collapsed–expanded transition as the concentration of the cosolvent (alcohol) increases. One possible explanation of the co-non-solvency phenomenon is the competition between the two solvents that cooperatively bind to the chain backbone,<sup>[17]</sup> another one could be linked to the very small incompatibility of the two solvents.<sup>[18]</sup> Moreover, it has been discussed in the previous literature<sup>[19]</sup> that the insolubility of ELPs is dependent on the alcohol hydrophobicity: the larger the alcohol hydrophobicity (following the sequence methanol, ethanol, isopropanol, and 1-propanol) the earlier the onset of the insolubility of ELPs. Apart

## 1. Introduction

Proline *cis/trans* isomerization plays an important role in the regulation of protein activities, such as protein folding,<sup>[1]</sup> the dynamics of signal response<sup>[2]</sup> and gene expression.<sup>[3]</sup> It may be also associated with human diseases, for example *cis* tau protein has been found as a major early driver of the progressive neurodegeneration after injury.<sup>[4]</sup> Though the cyclic side group of proline stabilizes both its *cis* and *trans* isomers, most prolyl peptide bonds in nature adopt the *trans* configuration.<sup>[5]</sup> The interconversion between the *cis* and *trans* isomers is a slow rate-limiting process

Y. Zhao, K. Kremer

Max Planck Institute for Polymer Research  
Ackermannweg 10, Mainz 55128, Germany  
E-mail: k.kremer@mpip-mainz.mpg.de

 The ORCID identification number(s) for the author(s) of this article can be found under <https://doi.org/10.1002/marc.202100907>

© 2022 The Authors. Macromolecular Rapid Communications published by Wiley-VCH GmbH. This is an open access article under the terms of the Creative Commons Attribution-NonCommercial-NoDerivs License, which permits use and distribution in any medium, provided the original work is properly cited, the use is non-commercial and no modifications or adaptations are made.

DOI: 10.1002/marc.202100907

from solution qualities, the solvation behavior of ELPs in aqueous binary mixtures may be also tuned by proline isomerization at the sequence level. This question still remains open and it is our main goal to address in this work.

Herein, we will focus on single ELP chains in water-ethanol mixtures. Taking advantage of our recent work,<sup>[15]</sup> we consider an ELP sequence (VPGVG)<sub>30</sub> with four different *cis* proline percentage  $P_{cis}$  and position: i)  $P_{cis} = 0$  with all prolines are in the *trans* state (the all-*trans* case); ii)  $P_{cis} = 0.5$  and the *cis* proline residues are located in two separated blocks **cccccccccccccttttttttttttttttt** (the *hs-cis* case); iii) or they are perfectly mixed with *trans* isomers **ctctctctctctctctctctctctctctct** (the *hm-cis* case); iv)  $P_{cis} = 1.0$  (the all-*cis* case). Our results show that the initial expanded-collapsed conformational behavior disappears in the all-*cis* case, because *cis* isomers facilitate rather compact structures without ethanol molecules, i.e., in pure water. Moreover, our data indicate that the shift in solvation free energy of a given ELP sequence is, within the error bars, independent of proline isomerization. Nevertheless, we also observe that *cis* isomers prevent both the peptide-water and peptide-ethanol hydrogen bonding in water-ethanol mixtures.

## 2. Experimental Section

### 2.1. All-Atom Simulations

All-atom simulations of an ELP sequence (VPGVG)<sub>30</sub> was performed by using the GROMACS, version 5.1.2, molecular dynamics package<sup>[21]</sup> with the CHARMM36m force field<sup>[22]</sup> together with the TIP3P water model.<sup>[23]</sup> For ethanol molecules, their bonded and non-bonded interactions were described by the CHARMM36m parametrization. In our simulations, eight different values of ethanol concentrations  $x_e$  were considered:  $x_e = 0.0382$  (1 232 ethanol and 31 056 water), 0.0809 (2 464 ethanol and 28 000 water), 0.1292 (3 696 ethanol and 24 912 water), 0.1844 (4 928 ethanol and 21 792 water), 0.25 (6 160 ethanol and 18 526 water), 0.50 (12 320 ethanol and 12 320 water), 0.75 (18 480 ethanol and 6 160 water) and 1.0 (24 640 ethanol and 0 water). In case of pure water with  $x_e = 0.0$  (0 ethanol and 32 177 water), the simulation data have been taken from our previous work.<sup>[15]</sup>

The simulations were performed in the isothermal-isobaric (*NPT*) ensemble at  $T = 300$  K, at which the considered peptide (VPGVG)<sub>30</sub> in pure water is in the expanded state (its LCST transition temperature  $T_l \cong 305$  K<sup>[15]</sup> under the currently chosen force field). The temperature of the system was kept constant by a velocity rescaling thermostat<sup>[24]</sup> with a coupling constant of 1 ps, and the pressure of the system was kept at 1 bar using the Parrinello-Rahman-Andersen barostat<sup>[25]</sup> with a coupling constant of 2 ps. The LINCS algorithm<sup>[26]</sup> was used for bond constraints. The electrostatic interactions were simulated using the particle mesh Ewald (PME) algorithm.<sup>[27]</sup> The cutoff of the electrostatic and the van der Waals interactions were set to 1.4 nm. The equations of motion were integrated using the leap-frog integrator with a time step of 2 fs. For a given  $x_e$ , two independent trajectories were generated, each of them covering a time of 1  $\mu$ s.

### 2.2. Water-Ethanol Mixtures

Following the previous literature,<sup>[28]</sup> the miscibility of the water-ethanol mixtures was checked by using the Kirkwood-Buff integrals (KBI)<sup>[29]</sup>:

$$G_{ij} = 4\pi \int_0^\infty (g_{ij}^{\mu VT}(r) - 1)r^2 dr. \quad (1)$$

Here,  $g_{ij}^{\mu VT}$  is the radial distribution function of components  $i$  and  $j$  in the  $\mu VT$  (grand canonical) ensemble, which links the macroscopic thermodynamics of complex liquid mixtures directly to the microstructure of molecules obtained from simulations. The calculation of KBI in computer simulations of finite size boxes typically may suffer from the finite-size effects. To solve this problem, an efficient method<sup>[30]</sup> was developed to obtain accurate KBI in the thermodynamic limit from nanoscale molecular dynamics simulations. Our obtained KBI for water-ethanol mixtures is shown in Figure 1(a) (note that only one atom per molecule was taken in the calculation of  $G_{ij}$ : the oxygen atom from water molecules and the middle carbon atom from ethanol molecules). The peak locations for the water-water KBI  $G_{ww}$ , the water-ethanol KBI  $G_{we}$  and the ethanol-ethanol KBI  $G_{ee}$  were in good agreement with experimental data.<sup>[28]</sup> Note that for a given aqueous binary mixture, the agreement of KBI in peak position was more important than that in magnitude.<sup>[28]</sup> The total number density  $\rho$  of water-ethanol mixtures was also calculated as a function of  $x_e$ , see Figure 1(b). A density dip with a maximal relative deviation of 0.15 from the ideal mixture line was observed, which agreed well with previous literature.<sup>[31]</sup> This weak incompatibility has been shown to be crucial for the observation of co-solvency, i.e., the swelling of a polymer in a mixture of poor solvents.<sup>[18,31]</sup>

## 3. Results and Discussion

### 3.1. Conformational Behavior

We first focus on the conformational behavior of the peptide in water-ethanol mixtures. Figure 2(a) shows the gyration radius  $R_g$  (the detailed definition of  $R_g$  can be found in the Supporting Information) of (VPGVG)<sub>30</sub> as a function of ethanol concentration  $x_e$  in the four considered cases. One can see that in the all-*trans* case, the results of  $R_g$  reproduce the experimentally observed expanded-collapsed-expanded scenario in water-ethanol mixtures,<sup>[19]</sup> namely the co-non-solvency behavior. As  $x_e$  increases from  $x_e = 0.0$  to 1.0, the change of  $R_g$  can be divided into three stages: i)  $R_g$  decreases monotonically when  $x_e \leq 0.0809$ ; ii)  $R_g$  increases monotonically at  $0.0809 < x_e < 0.5$ ; iii)  $R_g$  remains nearly as a constant as  $x_e \geq 0.5$ . As discussed in the previous literature,<sup>[17,31]</sup> the rapid initial collapse in stage i) is a more characteristic signal of a first-order-like behavior, while the gradual expansion in stage ii) is closer to a continuous expansion. Moreover, we can detect a collapsed window in stages i) and ii) compared to the pure water case, i.e., the ethanol concentrations at which  $R_g$  is smaller than that in pure water. As one can see from Figure 2(a), this window is located at  $0 < x_e \leq 0.1292$ , which again is in a good agreement with the experimental data.<sup>[19]</sup> In stage iii), the value of  $R_g$  is  $\approx 20\%$  larger than that in pure water

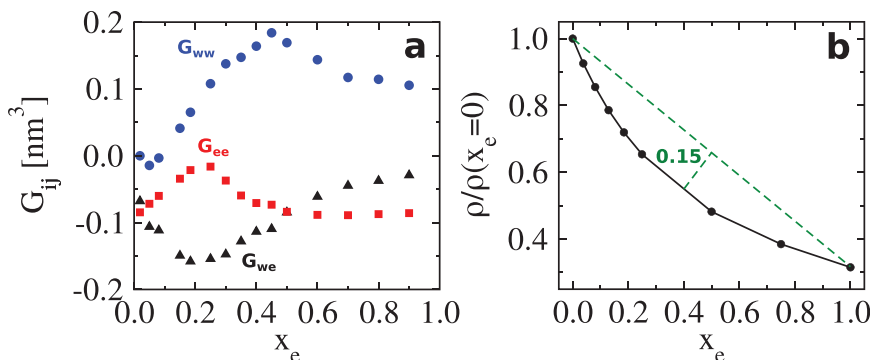


**Figure 1.** a) Kirkwood–Buff integrals for water–ethanol mixtures as a function of ethanol concentration  $x_e$ . b) Normalized total number density  $\rho/\rho(x_e = 0.0)$  of solvent molecules as a function of  $x_e$ . The green straight line is the linear interpolation between the data points of  $x_e = 0.0$  and 1.0.

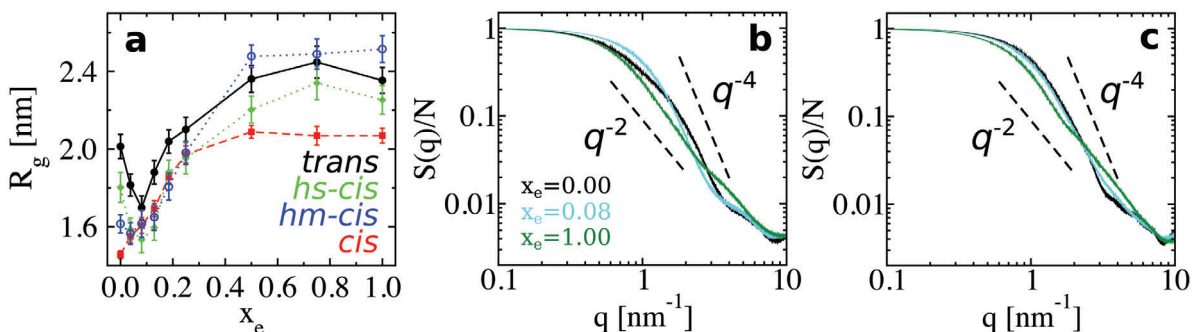


**Figure 2.** a)  $R_g$  of (VPGVG)<sub>30</sub> as a function of ethanol concentration  $x_e$  in the all-*trans* (black), *hs-cis* (green), *hm-cis* (blue) and all-*cis* (red) cases at  $T = 300$  K. b)  $S(q)$  in the all-*trans* case at  $x_e = 0.0$  (black), 0.0809 (cyan) and 1.0 (green). c) The same as panel (b) but for the all-*cis* case.

and is leveling off, which suggests that ethanol is a better solvent for the peptide compared to water. Note that the LCST transition temperature in the simulations of the peptide is 305 K,<sup>[15]</sup> and thus water is a good solvent at 300 K. The experimental LCST is 299 K,<sup>[32]</sup> which means that our simulations correspond to experiments at about 294 K. Typical snapshots of the peptide at different  $x_e$  can be found in Figure S2 in the Supporting Information.

However, the behavior for the all-*cis* case is markedly different, indicating that the conformational behavior of the peptide is strongly affected by proline isomerization. More specifically,  $R_g$  shows no stage i) in the all-*cis* case, i.e., there is no signature even of a weak collapse and the chain only experiences an expansion as  $x_e$  increases. The vanishing of an initial collapse may be because of the following reasons: a) the peptide is already tightly compact in pure water with  $x_e = 0.0$ , which leaves no space for further conformational shrinking as the solution quality changes; b) instead, the presence of ethanol slightly opens the ELP chain as a better solvent. At a first sight, our data suggest that the mechanism of peptide–ethanol interactions in the all-*cis* case is distinct from that in the all-*trans* case. In the mixed cases, the shape of  $R_g$  in the *hs-cis* case is similar to that in the all-*trans* case with the same window of shrinkage, though  $R_{g,hs-cis} < R_{g,all-trans}$  at all considered values of  $x_e$  because of the chain compactness in the half *cis* region (see Figure S3(a) in the Supporting Information). In the *hm-cis* case,  $R_g$  is nearly kept as a constant at  $x_e \leq 0.1292$ , which further supports the fact that the mechanism of *cis*-ethanol interactions might be different from that in the *trans* case. The value of  $R_g$  in the *hm-cis* case increases monotonically when  $0.1292 \leq$

$x_e < 0.5$ , and it is nearly a constant at  $x_e \geq 0.5$ . Note that it satisfies  $R_{g,hs-cis} < R_{g,all-trans} < R_{g,hs-cis} < R_{g,all-cis}$  at high ethanol concentration, which is determined by both the *cis* content-dependent effective backbone length<sup>[15]</sup> and the fraction of formed  $\beta$ -sheets (see Figures S2 and S4 in the Supporting Information) of the peptide. The longer effective backbone length and the less  $\beta$ -sheets formed along the backbone, the more expanded the chain is.

In order to better understand the conformational properties of the chain under proline isomerization, we have also plotted the Ramachandran plots of proline and its preceding valine residue in Figure S5 in the Supporting Information. Our data show that the flexibility of proline in both *trans/cis* states is similar to each other, however, the preceding valine is more flexible in the *cis* case. It seems that the steric rotation of *cis* proline leaves its preceding residue more space to act. A detailed analysis of the effects of proline isomerization on the activity of the preceding residues and its potential association with human diseases like neurodegenerative disorders will be the future directions.

To connect these more global results with characteristic length scale dependent polymer properties, we calculated the backbone structure factor  $S(q)$  (the definition of  $S(q)$  can be seen in the Supporting Information). The results for the all-*trans* case at  $x_e = 0.0$ , 0.0809 and 1.0 are shown in Figure 2(b) and in 2(c) for the all-*cis* case, respectively. The comparison between the two cases at different  $x_e$  is shown in Figure S6 in the Supporting Information. Though  $S(q)$  for the two cases looks quite similar at a first glance, there are a few significant differences. For  $x_e = 1.0$  on large distances, i.e. low  $q$  values, we obtain a  $q^{-2}$  power law indicating

an approximate Gaussian conformation. For the all-*cis* case this holds all the way down to distance of about  $2\pi/q \approx 0.8$  nm, corresponding to  $q \approx 8$  nm<sup>-1</sup>, which is slightly below a nm, where the slope becomes smaller, indicating a significant local stiffening. For the all-*trans* case we observe a much weaker deviation from the Gaussian behavior toward a more expanded structure already at a lower  $q$  of about 2.5 nm<sup>-1</sup>, corresponding to a distance of about 2.5 nm. This perfectly corresponds to the results obtained for  $R_g$ . In contrast, at zero ethanol content an extended stiff region ( $S(q) \propto q^{-1}$ ) on scales below about 2 nm is observed for both cases, which probably can be connected to the  $\beta$ -sheets formed (see Figure S4 in the Supporting Information and also the relative discussions in our previous work<sup>[15]</sup>). At smaller  $q$  values a slope between  $q^{-3}$  and  $q^{-4}$  is observed, an indication of an overall globular structure with a lower internal density for the all-*trans* case. Interestingly, for  $x_e = 0.0809$  the shifts compared to the  $x_e = 0.0$  case occur in a qualitatively different way for the two cases. While the shrinking of the all-*trans* chain is clearly observed at large scales, the local structure below about 2.5 nm remains almost unaltered. For the all-*cis* case, however, the global conformation remains almost unchanged and shifts occur below 2.5 nm. The missing initial expanded–collapsed conformational change in the all-*cis* chain as  $x_e$  increases from 0.0 to 0.0809 is the main difference between the two cases. These observations are also supported by the separate  $S(q)$  analysis of the *trans* and *cis* parts in the *hs-cis* case, as it is shown in Figure S7 in the Supporting Information. The large shrinking of the all-*trans* chain is connected to the reduction of the fraction  $f_\beta$  of  $\beta$ -sheets, while  $f_\beta$  in the all-*cis* case remains close to zero at all considered  $x_e$  (Figure S4 in the Supporting Information). It has to note that  $f_\beta$  in the all-*trans* case rises again as  $x_e$  increases until it reaches about 12% at  $x_e = 1.0$  in accord with the larger  $R_g$  value compared to the all-*cis* chain. The changes in  $f_\beta$  for the two cases considered are in line with the results of  $S(q)$  discussed above.

### 3.2. Solvation Free Energy

The Kirkwood–Buff (KB) fluctuation theory<sup>[29]</sup> is a classical approach to explore the thermodynamic properties of liquid mixtures. It links the thermodynamic properties of a solution to its microscopic structural quantities obtained from simulations. For any binary mixtures of solvent (s) and cosolvent (c), the solvation free energy of the peptide (p) can be calculated as:

$$\lim_{\rho_p \rightarrow 0} \left( \frac{\partial \Delta G}{\partial x_c} \right)_{p,T} = \frac{(\rho_s + \rho_c)^2}{\eta} (G_{ps} - G_{pc}). \quad (2)$$

Here,  $\rho_p \rightarrow 0$  indicates that the expression is derived for peptide systems at infinite dilution, which means a single chain in our case.  $\rho_s$  and  $\rho_c$  are the solvent and cosolvent number densities at pressure  $p$  and temperature  $T$ .  $G_{ij}$  is the KBI for components  $i$  and  $j$  (see Equation (1)), and  $x_c$  is the cosolvent concentration (the cosolvent is ethanol in our case, and thus  $x_c = x_e$ ).  $\eta = \rho_s + \rho_c + \rho_s \rho_c (G_{ss} + G_{cc} - 2G_{sc})$ , which measures the miscibility of the mixtures.

Figure 3 shows the solvation free energy shift  $\Delta G$  of (VPGVG)<sub>30</sub> in water-ethanol mixtures as a function of  $x_e$ . Interestingly,  $\Delta G$  in all four considered cases are the same within

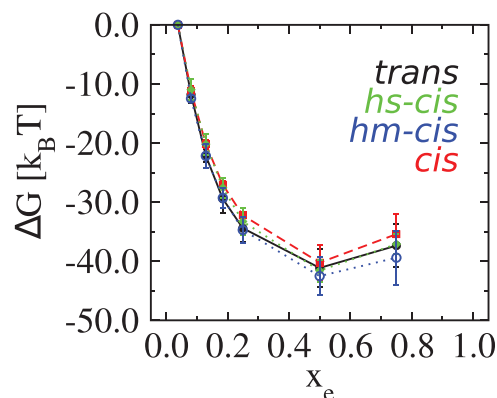


Figure 3. Shift in solvation free energy  $\Delta G$  of (VPGVG)<sub>30</sub> as a function of  $x_e$  in the all-*trans* (black), *hs-cis* (green), *hm-cis* (blue) and all-*cis* (red) cases at  $T = 300$  K.

the error, which indicates that proline isomerization does not contribute to the shift in the solvation free energy, despite the huge conformational differences. In other words, the solvation free energy of a peptide in aqueous ethanol mixtures is solely determined by the amino acid sequence itself. The understanding of this observation may be straightforward: the solvation free energy is dominated by the relative solvent and cosolvent interactions (the term  $G_{ps} - G_{pc}$  in Equation (2)), which is intimately linked to the amino acid sequence of the chain and coupled to local short length scale properties. This is supported by the  $S(q)$  results, which differed the least on small length scales. From Figure 3, we also observe a monotonically decreasing  $\Delta G$  within the range  $0 < x_e < 0.5$ , which again shows that ethanol is a better solvent for the peptide than water. However, there seems to be a slight increase of  $\Delta G$  as  $x_e \geq 0.5$ , indicating that the current amino acid sequence prefers a mixed solvent. Future work is needed to investigate this in detail.

### 3.3. Hydrogen Bonding

To characterize the peptide-(co)solvent affinity, we perform a hydrogen bonding analysis. Figures 4(a–b) show the results of the normalized proline–water  $N_{pro,w}/N_p$  and proline–ethanol  $N_{pro,e}/N_p$  hydrogen bonds (H-bonds),  $N_p = 30$  being the number of proline residues in the sequence. The total peptide-(co)solvent H-bonds can be found in Figure S8 in the Supporting Information, they have very similar shapes as the proline-(co)solvent ones. Our first observation is that as  $x_e$  increases, the value of  $N_{pro,w}/N_p$  decreases and that of  $N_{pro,e}/N_p$  increases as expected. For a given  $x_e$ , the all-*trans* case has the most proline-(co)solvent H-bonds, while the all-*cis* case has the least. These data suggest that the *cis* isomers suppress both the peptide–water and peptide–ethanol affinity of the ELP in water-ethanol mixtures (see also Figure S3(b) and (c) in the Supporting Information). The reduced solvent-accessible surface area (SASA) of the peptide in the all-*cis* case is the main cause of its decreased peptide-(co)solvent affinity, as it is shown in Figure S9 in the Supporting Information.

We have also determined the intramolecular  $N_{pro,np}$  H-bonds between the proline and non-proline (np) residues, see Figure S10(a) in the Supporting Information. We found that the *cis*

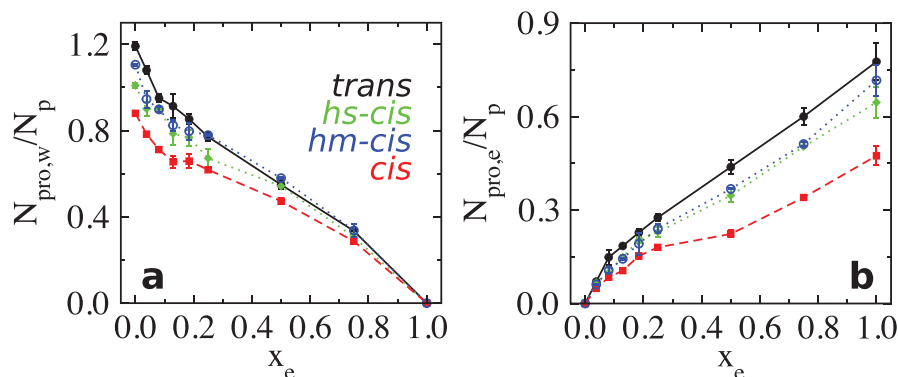


**Figure 4.** a) Normalized proline–water  $N_{pro,w}/N_p$  and b) proline–ethanol  $N_{pro,e}/N_p$  H-bonds by the number of proline residues  $N_p = 30$  as a function of  $x_e$  in the all-*trans* (black), *hs-cis* (green), *hm-cis* (blue) and all-*cis* (red) cases at  $T = 300$  K.

isomers promote intramolecular H-bonds in water-ethanol mixtures just as in pure water: the value of  $N_{pro,np}/N_p$  in the all-*cis* case is  $\approx 3$  times larger than that for the all-*trans* case at all considered  $x_e$ . The values for the two mixed *trans*, *cis* cases are in-between the former two extremes. However, concerning conformational aspects, intramolecular H-bonds formed in the all-*cis* case are very different from those in the all-*trans* case. This is demonstrated by the distance between pairs of residues (each pair forms a  $N_{pro,np}$  H-bond) separated by  $|i - j|$  residues along the chain (see Figure S10(b) in the Supporting Information). Our data show that all-*trans* chains on average have longer contour distance intramolecular H-bonds because of the formed  $\beta$ -sheets, while only local H-bonds are available in the all-*cis* case.

#### 4. Conclusion

We have studied the solvation behavior of an ELP sequence (VPGVG)<sub>30</sub> with four different *cis* compositions in aqueous ethanol mixtures. Our all-atom simulations reproduced the co-non-solvency phenomenon with an expanded–collapsed–expanded conformational transition in the all-*trans* case. The detected collapsed window is located at  $0 < x_e \leq 0.1292$ , which is in good agreement with the experimental results. Yet in the all-*cis* case, no initial collapse of the chain has been observed. Chains containing only *cis* isomers already display a very compact structure in pure water. Instead, the presence of ethanol molecules with low concentration can slightly open the all-*cis* chain. Furthermore, our data have shown that *cis* isomers reduces both the peptide–water and peptide–ethanol interaction affinities, though proline isomerization seemingly has no effects on the shift in solvation free energy of a given ELP sequence. Details of the microscopic origin of the initial collapse of the all-*trans* chains remain to be understood. The shift in solvation free energy by adding ethanol to water shows that the collapse occurs, despite the fact that the solvent quality becomes better. This suggests a classical co-nonsolvency scheme. However, for that the shift in solvation free energy seems to be too small.<sup>[31]</sup> Alternatively, the weak incompatibility of the two solvents, or more generally the three body effects might play a role.<sup>[18,33]</sup> This, however is beyond the scope of this initial study.

Our observation that proline isomerization plays a role in the solvation behavior of ELPs in aqueous ethanol mixtures, sheds

some light on the relevance of conformations on materials properties. This certainly should be taken into account if future applications of ELPs are considered.

#### Supporting Information

Supporting Information is available from the Wiley Online Library or from the author.

#### Acknowledgements

The authors thank Joseph F. Rudzinski and Aysenur Iscen for critical reading of our manuscript. This work was supported by European Research Council under the European Union's Seventh Framework Programme (FP7/2007-2013)/ERC Grant Agreement No. 340906-MOLPROCOMP. The authors dedicate this work to Rudolf Zentel. K.K. acknowledges many fruitful and enjoyable discussions and interactions over many joint years in Mainz.

Open access funding enabled and organized by Projekt DEAL.

#### Conflict of Interest

The authors declare no conflict of interest.

#### Data Availability Statement

The data that support the findings of this study are available from the corresponding author upon reasonable request.

#### Keywords

aqueous binary mixtures, *cis/trans* proline isomerization, elastin-like polypeptides (ELPs), stimulus-triggered polymeric phase behavior

Received: December 22, 2021

Revised: February 2, 2022

Published online: February 20, 2022

[1] W. J. Wedemeyer, E. Welker, H. A. Scheraga, *Biochemistry* **2002**, *41*, 14637.

- [2] P. Sarkar, C. Reichman, T. Saleh, R. B. Birge, C. G. Kalodimos, *Mol. Cell* **2007**, 25, 413.
- [3] C. J. Nelson, H. Santos-Rosa, T. Kouzarides, *Cell* **2006**, 126, 905.
- [4] A. Kondo, K. Shahpasand, R. Mannix, J. Qiu, J. Moncaster, C. H. Chen, Y. Yao, Y. M. Lin, J. A. Driver, Y. Sun, S. Wei, *Nature* **2015**, 523, 431.
- [5] C. Dugave, L. Demange, *Chem. Rev.* **2003**, 103, 2475.
- [6] D. Kern, M. Schutkowski, T. Drakenberg, *J. Am. Chem. Soc.* **1997**, 119, 8403.
- [7] F. Zosel, D. Mercadante, D. Nettels, B. Schuler, *Nat. Commun.* **2018**, 9, 3332.
- [8] A. Valiaev, D. W. Lim, T. G. Oas, A. Chilkoti, S. Zauscher, *J. Am. Chem. Soc.* **2007**, 129, 6491.
- [9] M. Mutter, T. Wöhr, S. Gioria, M. Keller, *Peptide Sci.* **1999**, 51, 121.
- [10] L. S. Sonntag, S. Schweizer, C. Ochsenfeld, H. Wennemers, *J. Am. Chem. Soc.* **2006**, 128, 14697.
- [11] G. Fischer, F. X. Schmid, *Biochemistry* **1990**, 29, 2205.
- [12] S. Fluegel, K. Fischer, J. R. McDaniel, A. Chilkoti, M. Schmidt, *Biomacromolecules* **2010**, 11, 3216.
- [13] S. Roberts, M. Dzuricky, A. Chilkoti, *FEBS Lett.* **2015**, 589, 2477.
- [14] F. G. Quiroz, A. Chilkoti, *Nat. Mater.* **2015**, 14, 1164.
- [15] Y. Zhao, K. Kremer, *J. Phys. Chem. B* **2021**, 125, 9751.
- [16] M. A. C. Stuart, W. T. Huck, J. Genzer, M. Müller, C. Ober, M. Stamm, G. B. Sukhorukov, I. Szleifer, V. V. Tsukruk, M. Urban, F. Winnik, *Nat. Mater.* **2010**, 9, 101.
- [17] D. Mukherji, C. M. Marques, K. Kremer, *Nat. Commun.* **2014**, 5, 4882.
- [18] D. Mukherji, C. M. Marques, T. Stuehn, K. Kremer, *Nat. Commun.* **2017**, 8, 1374.
- [19] C. E. Mills, E. Ding, B. D. Olsen, *Biomacromolecules* **2019**, 20, 2167.
- [20] Y. Zhao, M. K. Singh, K. Kremer, R. Cortes-Huerta, D. Mukherji, *Macromolecules* **2020**, 53, 2101.
- [21] M. J. Abraham, T. Murtola, R. Schulz, S. Páll, J. C. Smith, B. Hess, E. Lindahl, **2015**, 1, 19.
- [22] J. Huang, S. Rauscher, G. Nawrocki, T. Ran, M. Feig, B. L. de Groot, H. Grubmüller, A. D. MacKerell, Jr, *Nat. Methods* **2017**, 14, 71.
- [23] W. L. Jorgensen, J. Chandrasekhar, J. D. Madura, R. W. Impey, M. L. Klein, *J. Chem. Phys.* **1983**, 79, 926.
- [24] G. Bussi, D. Donadio, M. Parrinello, *J. Chem. Phys.* **2007**, 126, 014101.
- [25] M. Parrinello, A. Rahman, *Phys. Rev. Lett.* **1980**, 45, 1196.
- [26] B. Hess, H. Bekker, H. J. Berendsen, J. G. Fraaije, *J. Comp. Chem.* **1997**, 18, 1463.
- [27] U. Essmann, L. Perera, M. L. Berkowitz, T. Darden, H. Lee, L. G. Pedersen, *J. Chem. Phys.* **1995**, 103, 8577.
- [28] A. Perera, F. Sokolić, L. Almasy, Y. Koga, *J. Chem. Phys.* **2006**, 124, 124515.
- [29] J. G. Kirkwood, F. P. Buff, *J. Chem. Phys.* **1951**, 19, 774.
- [30] R. Cortes-Huerta, K. Kremer, R. Potestio, *J. Chem. Phys.* **2016**, 145, 141103.
- [31] D. Mukherji, C. M. Marques, K. Kremer, *Annu. Rev. Condens. Matter Phys.* **2020**, 11, 271.
- [32] D. T. McPherson, J. Xu, D. W. Urry, *Protein Expr. Purif.* **1996**, 7, 51.
- [33] J. U. Sommer, *Macromolecules* **2017**, 50, 2219.